AGU PUBLICATIONS

Geophysical Research Letters

RESEARCH LETTER
10.1002/2015GL067056

Key Points:
- In the lab instantaneous dynamic triggering requires fault gouge and dynamic strains exceeding 10−6
- Following triggering there is a recovery process that takes place over multiple stick-slip cycles
- We posit that similar processes may take place in situ

Supporting Information:
- Figures S1–S4

Correspondence to:
P. A. Johnson,
paj@lanl.gov

Citation:
Johnson, P. A., J. Carmeliet, H. M. Savage, M. Scuderi, B. M. Carpenter, R. A. Guyer, E. G. Daub, and C. Marone (2016), Dynamically triggered slip leading to sustained fault gouge weakening under laboratory shear conditions, *Geophys. Res. Lett.*, *42*, doi:10.1002/2015GL067056.

Received 1 DEC 2015
Accepted 1 FEB 2016
Accepted article online 4 FEB 2016

Dynamically triggered slip leading to sustained fault gouge weakening under laboratory shear conditions

P. A. Johnson[1], J. Carmeliet[2,3], H. M. Savage[4], M. Scuderi[5], B. M. Carpenter[6], R. A. Guyer[1], E. G. Daub[7], and C. Marone[5,8,9]

[1]Los Alamos National Laboratory, Geophysics Group, Los Alamos, New Mexico, USA, [2]Swiss Federal Institute of Technology Zürich (ETHZ), Zürich, Switzerland, [3]Swiss Federal Laboratories for Materials Science and Technology (Empa), ETH Domain, Zürich, Switzerland, [4]Lamont-Doherty Earth Observatory, Palisades, New York, USA, [5]Nazionale de Geofisica e Vulcanologia, Rome, Italy, [6]School of Geology and Geophysics, University of Oklahoma, Norman, Oklahoma, USA, [7]Center for Earthquake Research and Information, University of Memphis, Memphis, Tennessee, USA, [8]Department of Geosciences, Pennsylvania State University, University Park, Pennsylvania, USA, [9]Dipartimento Scienze della Terra, Università Sapienza di Roma, Rome, Italy

Abstract We investigate dynamic wave-triggered slip under laboratory shear conditions. The experiment is composed of a three-block system containing two gouge layers composed of glass beads and held in place by a fixed load in a biaxial configuration. When the system is sheared under steady state conditions at a normal load of 4 MPa, we find that shear failure may be instantaneously triggered by a dynamic wave, corresponding to material weakening and softening if the system is in a critical shear stress state (near failure). Following triggering, the gouge material remains in a perturbed state over multiple slip cycles as evidenced by the recovery of the material strength, shear modulus, and slip recurrence time. This work suggests that faults must be critically stressed to trigger under dynamic conditions and that the recovery process following a dynamically triggered event differs from the recovery following a spontaneous event.

1. Introduction

Dynamic earthquake triggering in the aftershock region and far field, first observed in response to the 1992 *M*7.3 Landers earthquake [*Hill et al*., 1991], is now established as a common phenomenon [e.g., *Brodsky and van der Elst*, 2014; *Gomberg and Johnson*, 2005; *Prejean and Hill*, 2011; *Velasco et al*., 2008; *Hernandez et al*., 2014]. In the context of a rate-state friction framework, *Voisin* [2001, 2002] suggested that triggering can inform us regarding general frictional properties. Indeed, based on laboratory [e.g., *Johnson et al*., 2008, 2012] and field studies [e.g., *Brodsky and van der Elst*, 2014; *van der Elst et al*., 2013], it is speculated that dynamic triggering can be applied as a probe of the critical shear stress state preceding failure, under certain conditions that may be related to the ambient stress environment, in particular. However, the mechanisms responsible for dynamic triggering are speculative, making it challenging to apply triggering observations to better understand the process of earthquake nucleation and failure. Our goal in this work is to use laboratory observations to unravel the mechanisms of triggered slip and probe critical state behavior of slip.

Here we explore the effects of modestly large strain amplitude (order 10^{-6}) waves, similar to strains observed at regional distances from moderate- to large-magnitude earthquakes. We analyze the slip characteristics of material at 3–8 MPa normal loads but only show results for experiments conducted at 4 MPa as they are representative of the full range explored in our studies. Above 8 MPa the glass beads employed in the experiments as surrogate gouge material begin to break. We intentionally avoid this regime so that our ongoing discrete element modeling of these experiments may be conducted [e.g., *Ferdowsi et al*., 2013, 2014a, 2014b] as well as those of other groups [e.g., *Giacco et al*., 2012, 2015].

2. Experiment

We perform experiments using the biaxial testing apparatus shown in Figure 1 [e.g., *Marone*, 1998]. Two layers of simulated fault gouge, under constant normal stress, are subjected to a shear stress via a constant loading rate boundary condition. The simulated fault gouge is composed of silica glass, class IV spheres (dimension from 105 to 149 μm). The apparatus measures shear stress and frictional force due to the displacement of the center block via a load cell. Gouge layer thickness, load-point displacement, material shear strain, and acoustic

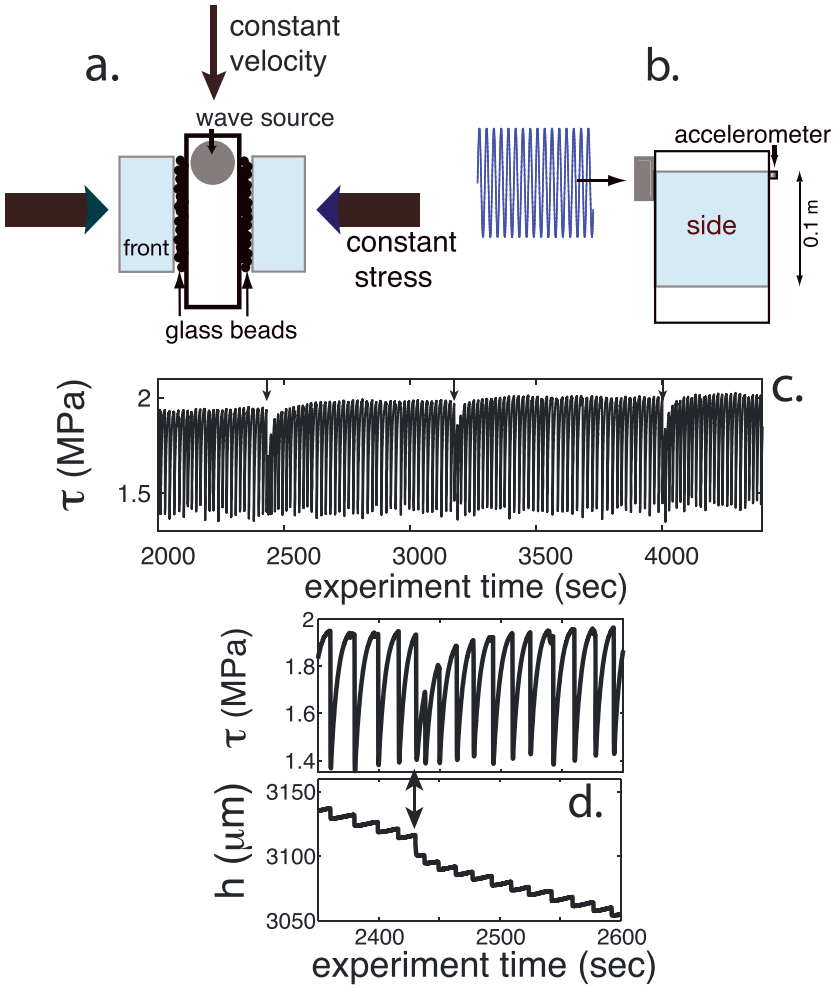

Figure 1. Experimental configuration (Experiment p1894). (a) We employ a double-direct shear configuration in a biaxial load frame, which applies a normal stress to three steel forcing blocks that contain symmetric layers of glass beads. An orthogonal piston drives the central block downward at a constant displacement rate to induce shear. The steel blocks have rough surfaces in contact with the glass beads. (b) The wave source transducer used for triggering applies a sinusoidal wave of duration of approximately 200 μs. An accelerometer placed on opposite sides of the central block detects the signal. (c) The recorded shear stress τ as a function of experimental run time. Three triggering episodes are shown as indicated by the vertical arrows. (d) Expanded view of the τ and combined layer thickness h of the two sheared layers. Trigger is shown by double arrow.

emission are also measured. The initial layer thickness is 2×4 mm, and the roughened interfaces with the drive block have dimensions 10 cm × 10 cm. The steel blocks have a velocity of order 5000 m/s. The center block is driven at a constant rate of 5 μm/s, corresponding to a strain rate of approximately 1.2×10^{-3}/s. The apparatus is servo-controlled so that constant normal stress and displacement rate of the drive block are maintained at ±0.1 kN and ±0.1 μm/s, respectively. The apparatus is monitored via computer to record all outputs at 10 kHz. Bulk friction is calculated from the measured shear stress divided by the applied normal stress. The geometry of the experimental setup maintains the central block parallel to the drive piston. When slip occurs, both gouge layers are weakened simultaneously as evidenced by the displacement measured on the central driving block.

Slip triggering is accomplished by applying acoustical tone bursts of order 200 μs from a large, 5 cm diameter custom-built piezoceramic (Matec, Inc), coupled to the central block applying vacuum grease and mechanically clamped in place. Tone burst strain amplitudes range from ~10^{-8} to 10^{-6}. The wavefield is directed parallel to the gouge layers which may or may not be optimal for fault triggering. We have not simulated the wavefield to study the complex interaction between it and the gouge layers. Acoustic emission is detected on the central block via a Brüel and Kjær model 4393 accelerometer and amplified by a Brüel and Kjær 2635 charge amplifier. From the measured acceleration of the detector $\ddot{u}$, the strain ε associated with both the triggering wave and

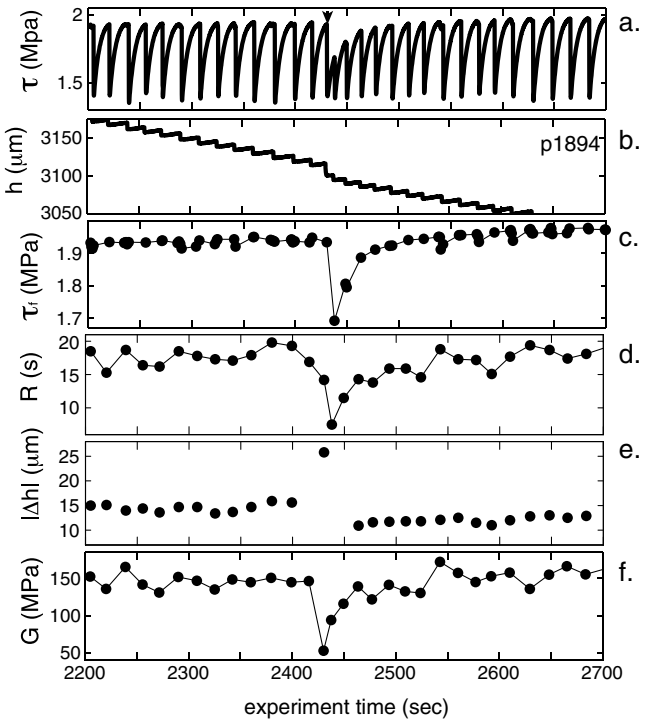

Figure 2. Effects of dynamic triggering on measured parameters for the first of three triggering episodes shown by vertical arrows in Figure 1c. (a) Shear stress τ, (b) layer thickness h, (c) shear stress at failure τ_f (the shear stress envelope), (d) recurrence (interevent) time R, (e) the absolute value of the change in layer thickness $|\Delta h|$, and (f) the quasi-static shear modulus G. At the triggering time, the shear stress, layer thickness, the recurrence interval, and the modulus abruptly decrease. Following this, the gouge material is weakened through multiple stick slip cycles as manifested by the recovery of the shear stress, recurrence, and modulus. The layer thickness behaves differently from the other measured quantities. There is an abrupt thinning of the gouge at the time of triggering corresponding to a large change in $|\Delta h|$, followed by what appears to be a permanent change. The recovery of the other parameters is not reflected in the layer thickness.

acoustic emission can be calculated from the particle velocity $\dot{u}$ and the layer wave speed c: $\varepsilon = \frac{\dot{u}}{c}$, where $\dot{u} = \frac{\ddot{u}}{\omega}$ and $\omega = 2\pi f$ [e.g., *Aki and Richards*, 2002]. The average measured wave speed in the granular material is approximately ~ 700 m/s, and frequency f is 40.3 kHz. We note that the gouge-block system facilitates wave energy to be trapped in the gouge layers potentially producing resonances that result in amplification. We are unable to observe this effect if it exists due to the strong resonance of the entire mechanical system, but we suggest that it may contribute to the triggering phenomenon we describe below.

3. Observations

In a typical experiment without triggering and subject to the conditions described above, the gouge layers undergo slide slip at regular time intervals and displacements that are characteristic of the fault dimension, applied load, and shearing rate (Figure 1c). (Due to the system stiffness, the central block does not stick but is always in motion—it does accelerate at slip time, thus is *slide slips*). At each slip event, the shear stress (and friction) precipitously decreases and the gouge layers abruptly undergo compaction (Figure 1d). Following the slip event, the gouge progressively dilates, simultaneous with an increase in shear stress, until the material reaches unstable conditions and the process repeats. For the experiment described below, we apply three successive triggering tone bursts of approximately 200 μs in duration. Each tone burst is well separated in time such that the material recovers to its initial, pretriggered bulk physical state as manifest by measured characteristics that will be described. We note that we are unable to trigger at precisely the same slip phase in successive triggering episodes because of the small variation in background slip recurrence, perhaps leading to variations in the aftermath. Figure 1c shows the shear stress as a function of time. The three triggering episodes are clearly observed as manifested by the perturbation on the maximum shear stress, which decreases at triggering time, and then progressively recovers. An expanded view of the triggering effect is shown in Figure 1d along with the layer thickness. The layers abruptly compact due to the triggering, considerably more than during a spontaneous slip event (Note that during a full experiment, the gouge layer thickness exhibits an overall thinning due to gouge material progressively being extruded into a bladder at the base of the sheared sample (Figure 1d). The thinning trend is clear in Figure 1d). Figures 2a–2f show, respectively, the measured shear stress τ, the layer thickness h, the shear stress at failure τ_f, the interevent or recurrence interval R, the absolute value of the change in the layer thickness during a failure event $|\Delta h|$, and the quasi-static shear modulus G. The shear modulus is obtained by measuring the tangent of the shear stress versus shear strain curves immediately following each slip event as described in Figure S1 in the supporting information.

We find that the triggered shear failure is instantaneous within the duration of the applied tone burst (~200 μs), forcing the gouge material into shear failure, as most clearly seen in Figures 1c, 1d, and 2. The shear stress

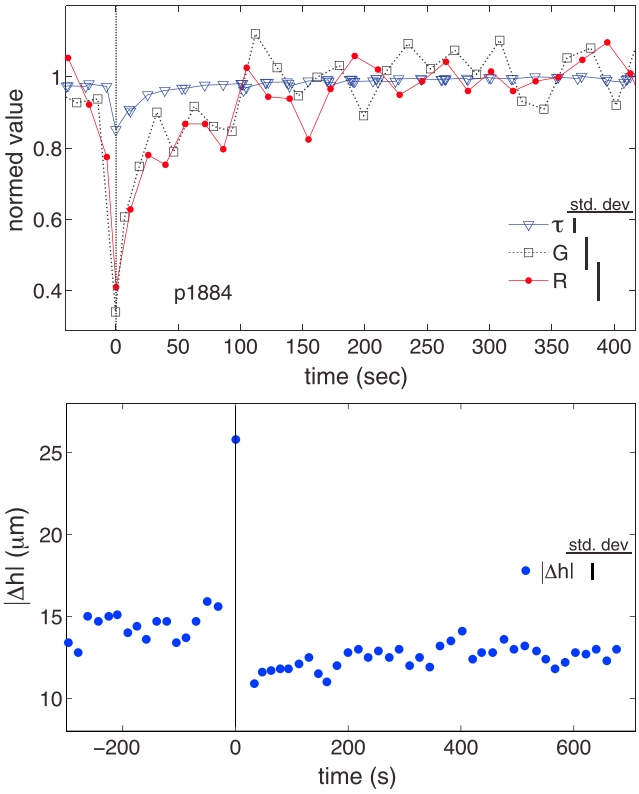

Figure 3. (a) Posttriggering behavior of the peak shear stress τ, quasi-static G recurrence interval R and (b) the change in layer thickness $|\Delta h|$. The standard deviations (excluding the change due to triggering) of each quantity are shown on the right-hand side of the figure. The τ, R, G, and $|\Delta h|$ data are normalized to their recovered values. Full recovery requires >200 s. (Figure 3b) Behavior of $|\Delta h|$ in response to the triggering wave (experiment p1894).

decreases by the same magnitude as that observed in spontaneous slip events (about 0.6 MPa), while the other measured parameters h, τ_f, R, and G exhibit a larger magnitude change than a spontaneous event. The induced compaction (Figures 1d and 2e) is order 10–15 μm, ~10% of a single bead diameter.

The horizontal load applied to the system influences the instantaneous triggering process. We observe instantaneous triggering over applied loads from 3 to 8 MPa (not shown but data available upon request). Below ~3 MPa we observe slow slip like fluidization as described in *Johnson et al.* [2012]. We have not explored the influence of wave frequency on dynamic triggering due to experimental constraints.

A second striking observation is that the modulus softening and frictional weakening following application of the tone burst persists through many slip cycles (Figures 1 and 2). Recovery takes place over a time interval of several 100 s, at which time the orderly behavior in τ_f, R, and G recover to their background behavior and/or magnitudes. We note that at strains below approximately 10^{-6} we are unable to trigger slip—it is only triggered when we exceed such dynamic strains and only when the material is in a critical shear stress state near failure. The critical state is also the region in which we observe acoustic precursors [*Johnson et al.*, 2013] corresponding to shear stress and frictional instability preceding failure. This region also corresponds to shear stress and frictional levels where microslips are observed in discrete element simulations [*Ferdowsi et al.*, 2013]. The results are load dependent. When the load is less than 3 MPa, we find that triggering can occur at any time in the slip cycle given strains 10^{-6} (e.g., Figure S3).

Due to the long-lived nature of the triggering-induced material weakening, our data can be used to examine the time-dependent recovery of granular friction following triggering. Frictional healing is traditionally measured using slide-hold-slide tests [e.g., *Marone*, 1998], while our experiments examine healing due to a triggering pulse that may induce failure and recovery over multiple failure cycles. In Figure 3a we show the normalized, recovery envelopes of τ, shear modulus G and recurrence interval R following the first triggering episode at approximately 2430 s in Figure 1c. The recoveries of τ, G and R appear to follow an approximate log(t) behavior (Figure S3a), but due to the discrete nature of the slip events, data are sparse immediately following triggering. The data also exhibit scatter that makes it difficult to quantify the exact temporal dependence. Figure 3b shows the effect of triggering on thickness change $|\Delta h|$. There is an induced strong, short-lived compaction following triggering but no apparent long recovery. There may be a permanent thickness change due to the shaking induced by the triggering episode and related material loss into the bladder. Figure S3b shows the recoveries for τ for all three applied perturbations. All three triggering tone bursts induce similar effects.

The dynamic triggering of failure is instantaneous within our ability to measure it, and we observe no dynamic wave amplitude effect on the triggering indicating that it is a threshold effect. That is, for small triggering strains less than ~10^{-7}, we observe no triggering. Above this dynamic strain, we observe triggering.

Further, we observe no affect on any of the measured parameters below this strain amplitude. We note that we have other such data sets at this same applied load that show the same behaviors described here—the observations are reproducible across the three triggering episodes in this experiment, as well as in other experiments conducted (not shown, but data available upon request).

4. Analysis and Discussion

We believe that the triggering is due to an instantaneous nonlinear elastic-induced softening and weakening of the bead pack due to the acoustical disturbance [e.g., *Johnson and Jia*, 2005]. This concept is essentially acoustic fluidization [e.g., *Melosh*, 1979, 1996; *Jia et al*., 2011]. The material fails because the shear modulus decreases precipitously (material softening), partially unjamming it (true unjamming requires $G = 0$). Three-dimensional numerical simulations of stick-slip of triggering show this effect in shearing simulations [*Giacco et al.,* 2015]. These simulations show that all of the particles participate in this process. In the experiment, we cannot determine whether or not all particles participate in the slip event. However, it is sufficient if fluidization takes place in a shear band leading to failure. The fact that the triggered stress drop resembles a spontaneous event, yet the other measured parameters exhibit triggered magnitudes larger than for a spontaneous event is puzzling. We anticipate that our ongoing DEM simulation effort will inform us as to why this is the case.

The remarkable observation of recovery of the measured characteristics following a triggering episode is difficult to understand. One might expect the successive slip event to erase the memory of the triggering wave, but this is not the case. A similar recovery of τ and h following triggering was observed at lower applied loads ($\leq$3 MPa) under stable sliding conditions [*Johnson et al*., 2012]. We cannot measure gouge particle displacements directly and again refer to simulations to study the particle-scale dynamics in order to gain insight into this process. In discrete element simulations in a sheared granular layer [*Ferdowsi et al*., 2014a], we observe that following triggering, the kinetic energy of the grains and the slipping contact ratio (ratio of the number of slipping contacts—those contacts in which the tangential contact force is at the Coulomb threshold—to the total number of contacts) remain elevated for some period of time following the wave perturbation. The shearing in the experiment and that in the simulation are different—in particular, the particle mass used in the simulation is much larger than in experiment. Despite this, we posit that contact instability induced by the acoustical perturbation may explain the long-lived material perturbation. Figure 4 illustrates our interpretation of the sequence of events. As the material fails, the force chains that bridge the shear band or full material are broken or disrupted. The chains reform rapidly postslip while the material behaves approximately elastically. As the shearing continues, the gouge begins to dilate, instability ensues (critical state), and the slip is repeated. When a dynamic wave is applied while the gouge is in the critical state, it breaks the force chains and induces early failure. Simultaneously, the wave vibration induces grain contact instability in terms of grain rotation and slipping contacts. The instability causes an overall weakening of the shear stress, friction, and shear modulus. In short, the material is partially (or entirely) fluidized, as directly measured by the quasi-static modulus decrease due to triggering. Because $G > 0$, it indicates that some force chains are broken by the triggering, but some thoroughgoing force chains remain that allow the material to continue to support a shear stress. Thus, the material softens as it weakens and compacts but does not lose all of its strength (We note that it is conceivable that all shear strength is briefly lost at triggering time, but the time resolution on our data is not sufficient to measure it.). The weakening persists as grain contacts displace or agitate, in analogy to thermal relaxation, to find their pre-triggering energy configurations, through multiple slip cycles. The induced weakening makes the material more prone to failure as evidenced by the shortened interevent time that progressively lengthens as contacts stabilize and force chains stabilize. Recent two-dimensional discrete element simulation work by *Reichhardt et al.* [2015] characterizing nonlinear behavior in disc packs supports the softening to weakening hypothesis, as do a number of experimental papers, including *Johnson and Jia* [2005] and *Brunet et al.* [2008]. These works suggest that disturbance of the force network is key to the process of failure.

Wave frequency may play and important role in the triggering process, and this is not addressed here. For instance, *van der Elst and Savage* [2015] observe triggering applying low-frequency waves in the same apparatus, but they observe no obvious recovery process. This potentially points to the importance of grain inertia in regard to the recovery process observed in the experiments presented here.

Our observations suggest that the nonlinear behavior of the fault gouge plays a dominant role in the triggering process. We investigate this further by attempting to trigger bare rock faces of westerly granite in multiple

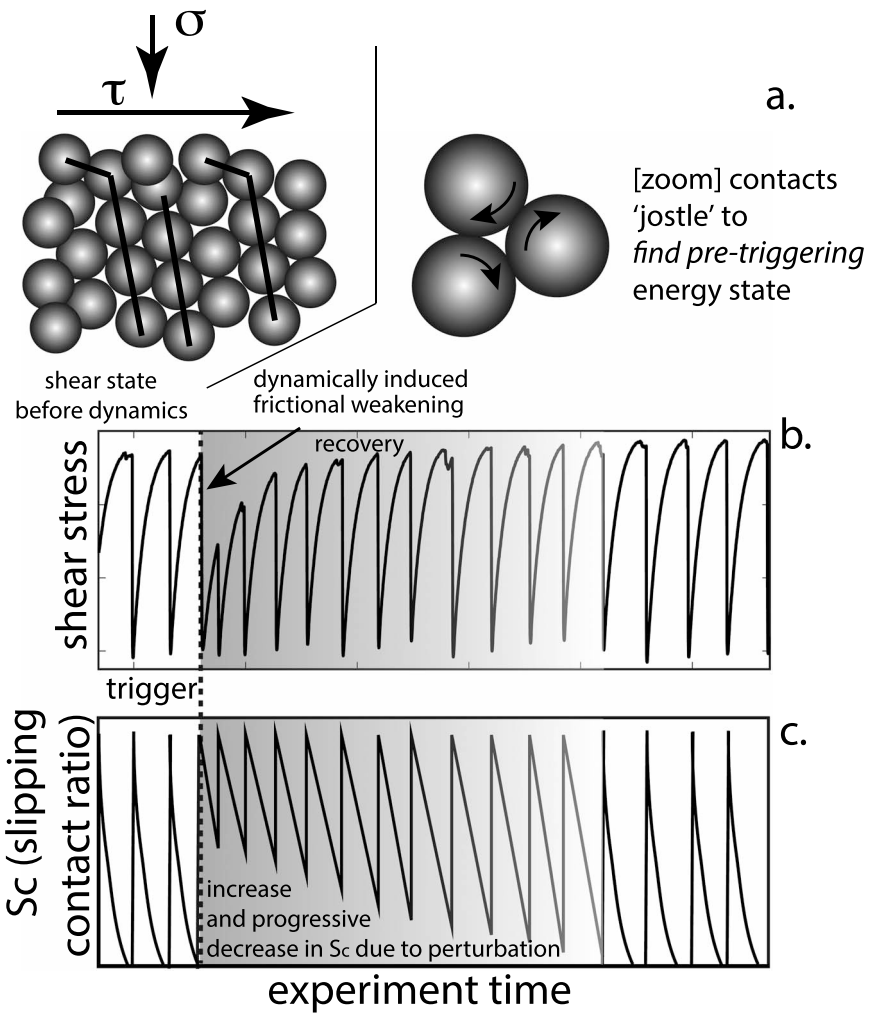

Figure 4. Cartoon illustrating dynamic induced instability. (a) The grain behavior preceding and following dynamic wave excitation. The material contains chains of force (dark lines) that maintain material strength. (b) The wave perturbation triggers the system, forcing an abrupt failure due to material softening and weakening (fluidization) by breaking force chains. (c) The slipping contact ratio S_c of stick-slip event preceding and following triggering. Following stick-slip, there is a S_c increase due to grain displacements that rapidly subsides. The effect of the wave perturbation is first to induce instantaneous slip and induce bulk shear and frictional weakening. This is due to dynamically induced contact instability placing the system into a different material state. Remarkably, the weakening persists through multiple stick-slip cycles until the contacts have found their pre-triggering energy configurations via thermal-like "jostling" of the contacts. The S_c evolution postslip is due to very small grain contact displacements rather than large rearrangement of grains.

experiments. We do not observe triggering under the same experimental conditions including the same triggering amplitudes as those described above (Figure S3). Clearly, at sufficiently large dynamic strains, triggering should take place when the Coulomb criterion is met [e.g., *Sobolev et al*., 1993], but the vibration-induced stresses examined here are much smaller than the absolute stress levels, highlighting the importance of the granular material in the triggering process. Our conclusion is that the presence of gouge material and its fragility is critical for both triggering and the recovery process to take place as shown in the conceptual model described in Figure 4.

In summary, based on our work to date, we observe dynamical triggering effects over applied load levels explored, ranging from 0.5 to 8 MPa. Below about 3 MPa the triggering may take place anywhere in the stress cycle and exhibit slow slip or fluidization characteristics, e.g., Figure S3 [see also *Johnson et al*., 2012]. Above 3 MPa, the triggered slip may be instantaneous with a long recovery of the measured characteristics, as shown here. Under conditions where acoustic perturbation is applied repeatedly and through multiple slip cycles, the system may exhibit delayed failures and marked perturbation to the interevent time and other measured characteristics [*Johnson et al*., 2008].

Instantaneous dynamic triggering is common in the Earth, suggesting that critically stress faults in Earth may exhibit similar effects to those seen in our laboratory experiments. Our experimental results suggest that the shaking from earthquakes can have a large impact on the fault core, leaving it in an evolving elastic state for long time periods following perturbation. Our work also supports the notion that triggered seismicity can provide new methods for examining and understanding the complex process of earthquake nucleation and triggering.

Acknowledgments

Data can be obtained directly from either P.J. or C.M. This work was supported by DOE Geothermal, NETL DOE LANS contract DE-AC52-06NA25396, and Institutional Support (LDRD) at Los Alamos to P.J. and R.G.; DOE EGS DE-EE0006762, NSF EAR 1520760 and IGPP (Institutional Support at LANL) to C.M., M.S., and B.C.; European Union Horizon 2020 656676 to M.S.; SCEC grant 13117 to H.S.; and Swiss National Science Foundation funding to J.C.

References

Aki, K., and P. Richards (2002), *Quantitative Seismology*, Univ. Sci. Books, Sausalito, Calif.

Brodsky, E., and N. van der Elst (2014), The uses of dynamic earthquake triggering, *Annu. Rev. Earth Planet. Sci.*, *42*, 317–339, doi:10.1146/annurev-earth-060313-054648.

Brunet, T., X. Jia, and P. Johnson (2008), Transitional, elastic-nonlinear behaviour in dense granular media, *Geophys. Res. Lett.*, *35*, L19308, doi:10.1029/2008GL035264.

Ferdowsi, B., M. Griffa, R. A. Guyer, P. A. Johnson, C. Marone, and J. Carmeliet (2013), Microslips as precursors of large slip events in the stick-slip dynamics of sheared granular layers: A discrete element model analysis, *Geophys. Res. Lett.*, *40*, 4194–4198, doi:10.1002/grl.50813.

Ferdowsi, B., M. Griffa. R. A. Guyer, P. A. Johnson, C. Marone, and J. Carmeliet (2014a), 3D discrete element modeling of triggered slip in sheared granular media, *Phys. Rev. E*, *89*(4), 042204, doi:10.1103/PhysRevE.89.042204.

Ferdowsi, B., M. Griffa, R. A. Guyer, P. A. Johnson, and J. Carmeliet (2014b), Effect of boundary vibration on the frictional behavior of a dense sheared granular layer, *Acta Mech.*, doi:10.1007/s00707-014-1136-y.

Giacco, F., E. Lippiello, and M. P. Ciamarra (2012), Solid-on-solid single-block dynamics under mechanical vibration, *Phys. Rev. E: Stat., Nonlinear, Soft Matter Phys.*, *86*, 016110.

Giacco, F., L. Saggese, L. de Arcangelis, E. Lippiello, and M. Pica Ciamarra (2015), Dynamic weakening by acoustic fluidization during stick-slip motion, *Phys. Rev. Lett.*, *115*, 128001.

Gomberg, J., and P. Johnson (2005), Dynamic triggering of earthquakes, *Nature*, *437*, 830, doi:10.1038/437830a.

Hernandez, S., E. Brodsky, and N. J. van der Elst (2014), The magnitude distribution of dynamically triggered earthquakes, *Geochem. Geophys. Geosyst.*, *15*, 3688–3697, doi:10.1002/2014GC005404.

Hill, D., et al. (1991), Seismicity remotely triggered by the magnitude 7.3 Landers, California, earthquake, *Science*, *260*, 1617–1623, doi:10.1126/science.260.5114.1617.

Jia, X., T. Brunet, and J. Laurent (2011), Elastic weakening of a dense granular pack by acoustic fluidization: Slipping, compaction, and aging, *Phys. Rev. E: Stat. Nonlinear Soft Matter Phys.*, *84*, 020301.

Johnson, P. A., and X. Jia (2005), Nonlinear dynamics, granular media and dynamic earthquake triggering, *Nature*, *437*, 871–874, doi:10.1038/nature04015.

Johnson, P. A., H. Savage, M. Knuth, J. Gomberg, and C. Marone (2008), The effect of acoustic waves on stick-slip behavior in sheared granular media: Implications for earthquake recurrence and triggering, *Nature*, *451*, 57–60, doi:10.1038/nature06440.

Johnson, P. A., B. Carpenter, M. Knuth, B. Kaproth, P. Le Bas, E. Daub, and C. Marone (2012), Nonlinear dynamical triggering of slow slip on simulated earthquake faults with implications to Earth, *J. Geophys. Res.*, *117*, B04310, doi:10.1029/2011JB008594.

Johnson, P. A., B. Ferdowsi, B. M. Kaproth, M. Scuderi, M. Griffa, J. Carmeliet, R. A. Guyer, P.-Y. Le Bas, D. T. Trugman, and C. Marone (2013), Acoustic emission and microslip precursors to stick-slip failure in sheared granular material, *Geophys. Res. Lett.*, *40*, 5627–5631, doi:10.1002/2013GL057848.

Marone, C. (1998), Laboratory-derived friction laws and their application to seismic faulting, *Annu. Rev. Earth Planet. Sci.*, *26*, 643–696.

Melosh, J. (1979), Acoustic fluidization: A new geologic process?, *J. Geophys. Res.*, *86*, 7513–7520, doi:10.1029/JB084iB13p07513.

Melosh, J. (1996), Dynamical weakening of faults by acoustical fluidization, *Nature*, *379*, 601–606, doi:10.1038/379601a0.

Prejean, S. G., and D. P. Hill (2011), Earthquakes, dynamic triggering of, in *Encyclopedia of Complexity and and Forecasting of Early Warning*, edited by R. A. Meyers, pp. 383–405, Springer, New York.

Reichhardt, C. J. O., L. M. Lopatina, X. Jia, and P. A. Johnson (2015), Softening of stressed granular packings with resonant sound waves, *Phys. Rev. E*, *92*, 022203, doi:10.1103/PhysRevE.92.022203.

Sobolev, G., H. Spetzler, A. Koltsov, and T. Cheldize (1993), An experimental study of triggered stick-slip, *Pure Appl. Geophys.*, *140*, 79–94.

van der Elst, J. J., H. M. Savage, K. M. Keranen, and G. A. Abers (2013), Enhanced remote earthquake triggering at fluid-injection sites in the midwestern United States, *Science*, *341*(6142), 164–167.

van der Elst, N. J., and H. M. Savage (2015), Frequency dependence of delayed and instantaneous triggering on laboratory and simulated faults governed by rate-state friction, *J. Geophys. Res. Solid Earth*, *120*, 3406–3429, doi:10.1002/2014JB011611.

Velasco, A., S. Hernandez, T. Parsons, and K. Pankow (2008), Global ubiquity of dynamic earthquake triggering, *Nat. Geosci.*, *1*, 375–379, doi:10.1038/ngeo204.

Voisin, C. (2001), Dynamic triggering of earthquakes: The linear slip-dependent friction case, *Geophys. Res. Lett.*, *28*, 3357–3360, doi:10.1029/2001GL013101.

Voisin, C. (2002), Dynamic triggering of earthquakes: The nonlinear slip-dependent friction case, *J. Geophys. Res.*, *107*(B12), 2356, doi:10.1029/2001JB001121.

Geophysical Research Letters

Supporting Information for

Dynamically triggered slip leading to sustained fault gouge weakening under laboratory shear conditions

P. A. Johnson,[1] J. Carmeliet,[2,3] H.M. Savage,[4] M. Scuderi,[5] B. D. Carpenter,[6] R. A. Guyer,[1] E. G. Daub,[7] and C. Marone[5,,8,9]

[1]Los Alamos National Laboratory, Geophysics Group, Los Alamos, USA, E-mail: paj@lanl.gov

[2]Swiss Federal Institute of Technology Zürich (ETHZ) – Wolfgang-Pauli-Strasse 15, CH-8093 Zürich, Switzerland

[3]Swiss Federal Laboratories for Materials Science and Technology (Empa), ETH Domain -Uberlandstrasse 129, CH-8600, Dübendorf (Zürich), Switzerland

[4]Lamont-Doherty Earth Observatory, 226 Seismology, 61 Route 9W- PO Box 1000, Palisades, NY 10964-8000

[5] Nazionale de Geofisica e Vulcanologia, Via di Vigna Murata, 605 00143 Rome, Italy

[6] School of Geology and Geophysics, University of Oklahoma, 100 E. Boyd St. Norman OK, 73019

[7]University of Memphis, Center for Earthquake Research and Information, 3890 Central Ave., Memphis, TN 38152, USA.

[8]Department of Geosciences, Pennsylvania State University, University Park, Pennsylvania 16802, USA

[9]Dipartimento Scienze della Terra, Università Sapienza di Roma, P.le A. Moro 5, 00185 Rome, Italy

Contents of this file

Introduction

Here we show additional plots of data from the experiment shown in the main text as well as experiments that were conducted under other conditions or employing other materials. We first show how the static shear modulus G is obtained. We follow this with post triggering recovery data plotted in semi-log format. Following this we show results of triggering at a lower applied

load level where triggering may take place anywhere in the slip cycle. Finally we show attempted triggering applying bare rock faces of crystalline rock. Here triggering fails supporting the conclusion that granular material is a necessary requirement for dynamic triggering to occur. All experiments were conducted under room dry conditions at ambient temperature.

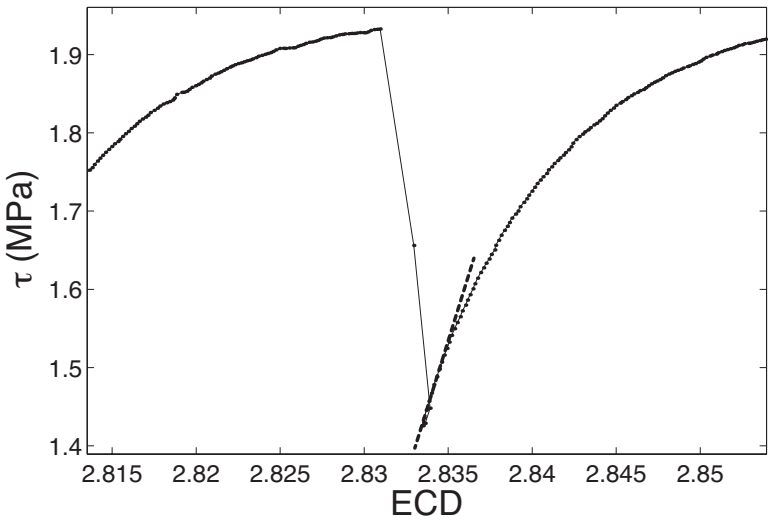

Figure S1. Measurement of tangent shear modulus G. Shear stress as a function of the elastically corrected displacement (ECD) of the driving ram. The stiffness G (MPa/u), where u is the ECD, is determined applying a linear fit to the data immediately following a shear failure (dashed line) while the gouge responds linearly and before dilation and nonlinear behavior ensues. This is the 'tangent stiffness. The stiffness is corrected for the known stiffness of the vertical load frame. The shear modulus is obtained by dividing by the layer thickness, so that G=K/h, where h = layer thickness.

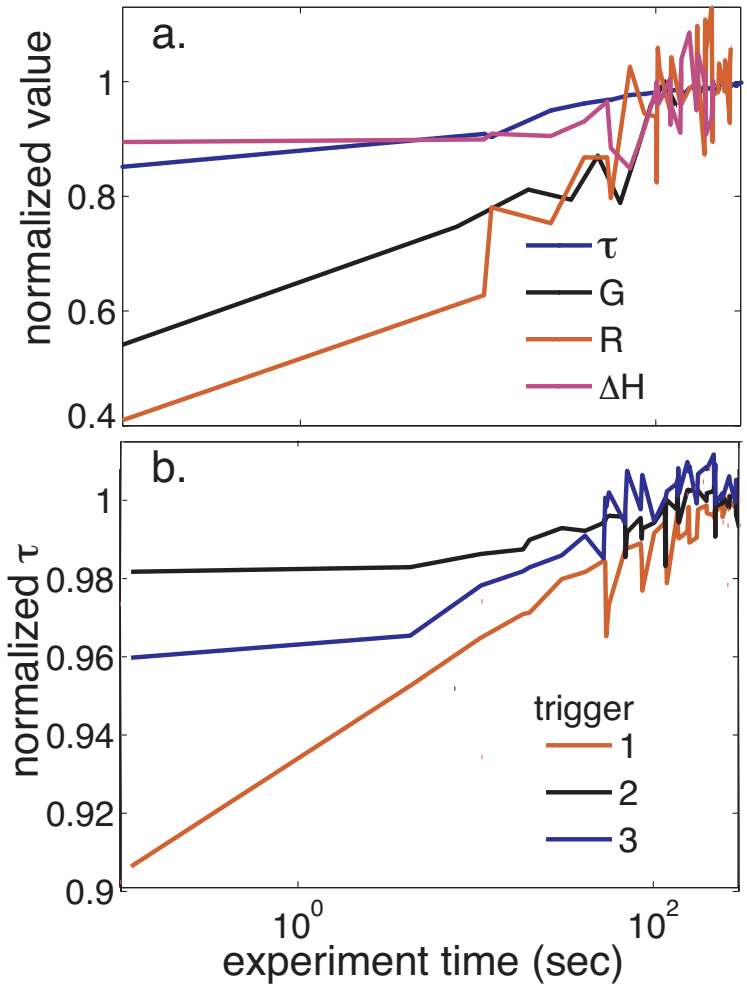

Figure S2. (a) Recoveries from post dynamic triggering of the peak shear stress t , the quasi-static modulus G, recurrence interval R, and the change in layer thickness |DH|. *G* is the quasi-static modulus obtained by in the manner described in S1. The t, R and |Dh| data are obtained by measuring the value just before slip takes place for each successive slip event following triggering. Data are normalized to their recovered values. Full recovery requires >200 seconds. (b) Recoveries of the shear stress at failure for the three triggering episodes shown in Figure 2.

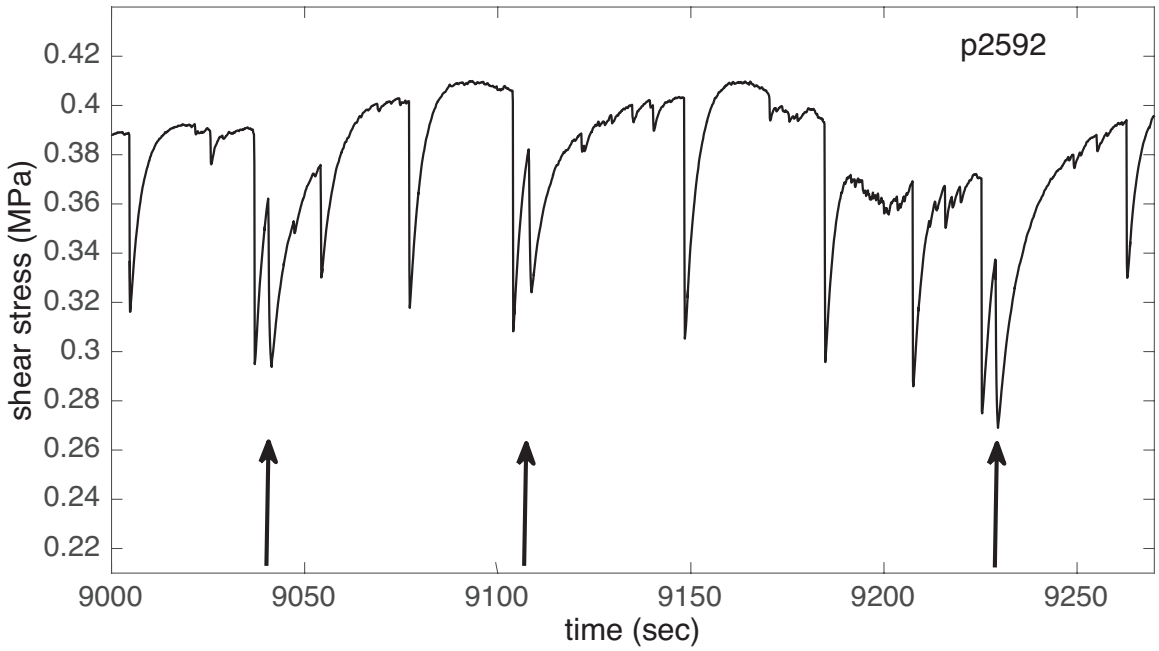

Figure S3. Triggering early in the earthquake cycle observed at small shear stress levels. The arrows indicate the trigger times. We find that at small applied horizontal loads (below 3 MPa), and for the dynamic strains employed in the experiments described in the main text, triggering can take place anywhere in MPa slip cycle in contrast to applied loads greater than 3 MPa where triggering only occurs when the system is in a critical state near failure.

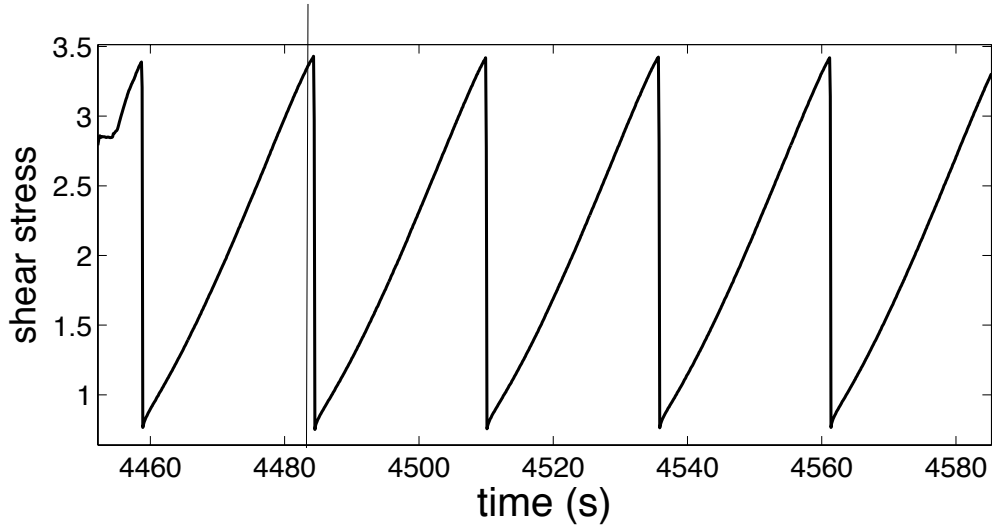

Figure S4. Attempted triggering in Westerly granite for experiment p1360 shown at location of vertical line near 448 seconds. There is no effect on the shear stress. Triggering is not induced at the dynamic strain levels applied for triggering elsewhere in this study.